# Experimental and numerical studies on penetration of shaped charge into concrete and pebble layered targets

# C Wang\*, W Xu, T Li

State Key Laboratory of Explosion Science and Technology, Beijing Institute of Technology, China

#### **ABSTRACT**

Experiments on penetrating into concrete and pebble layered targets were performed by shaped charge with different cone angles, liner wall thicknesses, length to diameter ratios and charge diameters at different standoffs. Based on the experimental data, the influence of shaped charge's structural parameters on crater diameter, hole diameter, crater depth and penetration depth was analyzed in detail. Meanwhile, formation and penetration processes of all shaped charges were simulated by AUTODYN software for investigating the more intrinsic mechanisms, in which the numerical models are the same as those set up in the experiments. The results obtained in this paper indicate that there are obvious differences between jetting projectile charge (JPC) and explosively formed projectile (EFP) in penetrating into multi-layer targets. For the same charge diameter, the values of hole diameter formed by EFP were much larger than JPC. However, for the same standoff, the penetration depth caused by JCP were larger than EFP. The interfacial effect exists in the penetration progress of JPC.

# 1. INTRODUCTION

Shaped charge penetrating into multi-layer targets is a complicated mechanical problem which usually involves shock wave propagation, dynamic behavior of multi-layer targets, interactions between different layers and so on. Most previous investigations focus on penetrating into pure concrete targets. In general, the theoretical researches focus on penetration depth and diameter in this field. A simplified calculation formula of penetration depth was presented by Brikhoff firstly [1]. Based on the virtual origin theory, Allison et al. provided the penetration depth by integral in jet length [2]. By modifying the Bernoulli formula of jet penetrating into targets [3], Tate et al. developed one-dimensional correction dynamic model [4]. Chou et al. calculated the total penetration depth by the jet's double linear velocity distribution instead of the nonlinear velocity distribution [5]. As for penetration diameter, Szendrei established an analytical model [6]. Held improved the Szendrei equation and performed experiments to validate the Szendrei/Held equation [7]. Wang et al. presented a calculation formula by modifying the hole enlargement pressure of Szendrei model [8]. In recent years, both numerical and experimental techniques have been utilized extensively to investigate concrete penetration [9-11]. Pincosy et al. studied the multiple shaped charge penetrating into concrete targets by numerical simulations and

<sup>\*</sup>Corresponding Author: wangcheng@bit.edu.cn

experiments [12]. Xiao et al. analyzed the shaped charge liner composed of copper and aluminum material penetrating into concrete targets [13]. Wang et al. investigated shaped charge penetrating into concrete targets experimentally, numerically and theoretically [14].

Investigations on shaped charge penetrating into multi-layer targets are far less than that of pure concrete targets. Due to lack of systematic experimental data, the intrinsic mechanisms of shaped charge penetrating into multi-layer targets are not clear up to now. So we carried out a series of experiments on penetrating into multi-layer targets by shaped charge with different cone angles, liner wall thicknesses, length to diameter ratios and charge diameters at different standoffs. Using both experiments and numerical simulations, we investigated the variation laws of crater diameter, hole diameter, crater depth and penetration depth with different geometric configurations of shaped charge and different standoffs.

#### 2. EXPERIMENTAL SCHEME

The charges with diameters of 70mm and 65mm are designed, composition B with density of  $1.6 \mathrm{g/cm^3}$  is selected as the main charge and the material of liners is steel in the experiments. As shown in Fig. 1, the height of charge with 70mm diameter is L=100mm. The cone angles of the liner are  $120^\circ$  and  $150^\circ$ , and wall thicknesses are uniformly 4mm and 5mm. Four kinds of standoffs (1D, 1.5D, 2D and 4D) are investigated respectively in this paper. Here the notation D is defined as charge diameter. Fig. 2 shows the schematic of shell. The parameters of the shaped charge with diameter of 70mm are  $\Phi_1 = 45 \mathrm{mm}$ ,  $\Phi_2 = 75 \mathrm{mm}$ ,  $\delta = 2.5 \mathrm{mm}$ ,  $\alpha = 45^\circ$ ,  $L_1 = 105 \mathrm{mm}$ ,  $L_2 = 11 \mathrm{mm}$  and  $L_3 = 141 \mathrm{mm}$ , respectively.



Figure 1: Shaped charge with diameter of 70mm.

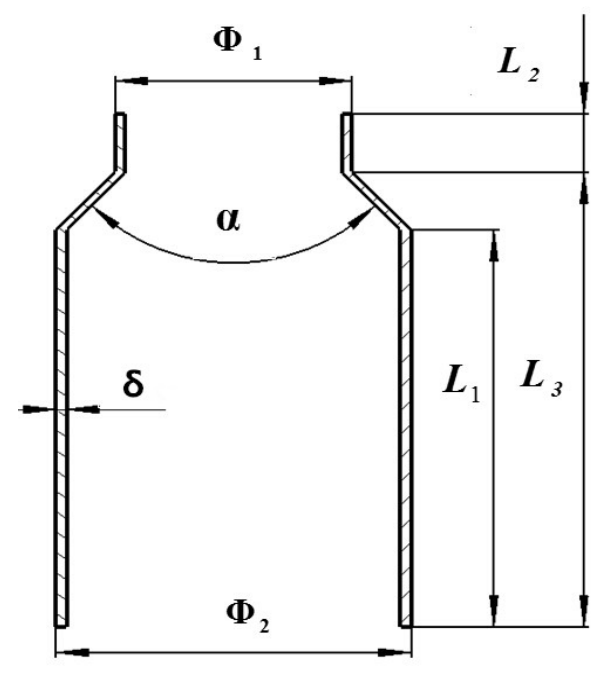


Figure 2: Schematic of shell.

Fig. 3 shows the shaped charge with diameter of 65mm. The heights of these charges are 54mm and 94mm, respectively. Two kinds of liners are used in the experiments, in which uniform liner wall thickness and the cone angle are 3mm and 120°, respectively; the other liner wall thicknesses are variable in a linear way, the top and bottom liner wall thicknesses are 1.8mm and 1.3mm respectively, the inner and external cone angles are 114° and 120° respectively. Fig. 4 shows part of shells with the charge diameter of 65mm. The heights of shells are L1=35mm, L3=65mm and L1=75mm, L3=105mm respectively; other parameters are  $\Phi_1 = 44$ mm,  $\Phi_2 = 69$ mm,  $\delta = 2$ mm,  $\alpha = 45$ ° and L2=11mm.



Figure 3: Shaped charge with diameter of 65mm.



Figure 4: Shells with diameter of 65mm.

The multi-layer targets consist of two layers in the experiments, as shown in Fig. 5. The upper layer is concrete. Its thickness is 400mm, the density 2.4g/cm<sup>3</sup> and the compressive strength 30MPa. The lower layer is pebble. Its thickness is 300mm and the largest diameter is 40mm.

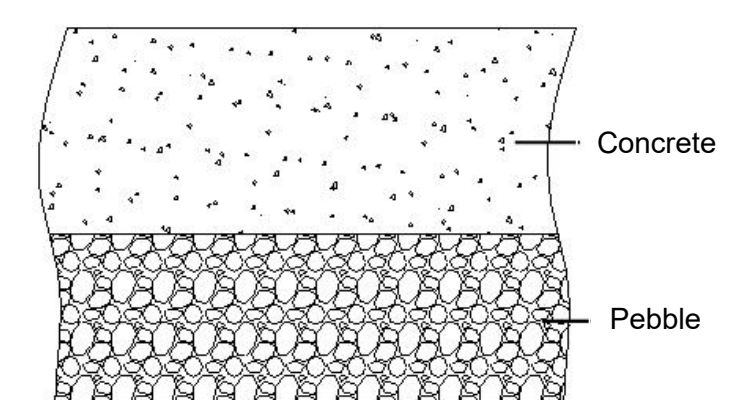


Figure 5: Schematic of multi-layer targets.

The experimental setups and results of different charge diameters are shown in Fig. 7. The values of crater diameter  $D_1$ , hole diameter  $D_2$ , crater depth  $H_1$  and penetration depth H are measured as shown in Fig. 6. The maximum and minimum values of  $D_1$  and  $D_2$  are recorded, and then the averages of maximum and minimum values are adopted to depict variation curves, as shown in Fig. 8 and Fig. 9.

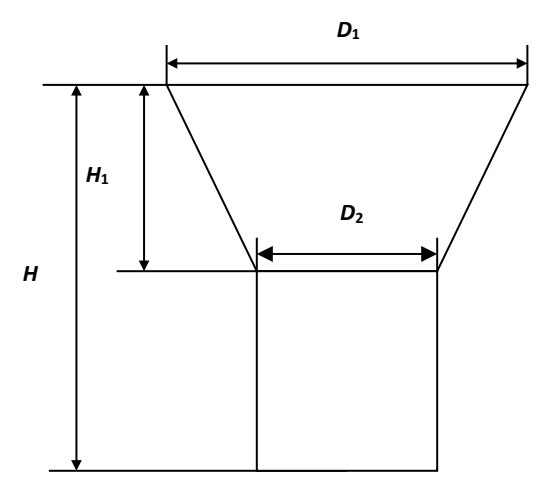


Figure 6: Damage parameters of targets.



Figure 7: The experimental setups and results of different charge diameters; (a) Experimental setups. (b) Experimental results.

# 3. THE RESULTS OF CHARGE DIAMETER 70MM

# 3.1. Results of Crater Diameter D<sub>1</sub>

Table 1 and Fig. 8 illustrate that, in the case of 120° cone angle, the crater diameter decreases with the increase of standoff, and the maximum value of crater diameter is 10.7D. Under the impact of the detonation wave, the liner moves inward and generates JPC. The JPC stretching and becoming thin with the increase of standoff causes the decrease of crater diameter. In the case of 150° cone angle, the liner overturning and extending under the action of explosion produces EFP. The maximum value of crater diameter formed by EFP is 9D. Under the condition of standoff higher than 2D and the same cone angle, the crater diameter formed by shaped charge with 4mm liner wall thickness is larger than 5mm liners wall thickness.

Table 1: Experimental results of crater diameter with different cone angles and liner wall thicknesses under different standoffs (mm)

Cone angle (°) Thickness (mm)		Standoff					
		1D	1.5D	2D	4D		
120	4	_	750×750	600×700	510×580		
	5	_	700×780	560×600	500×600		
150	4	410×420	_	500×500	610×650		
	5	440×580	_	400×430	400×500		

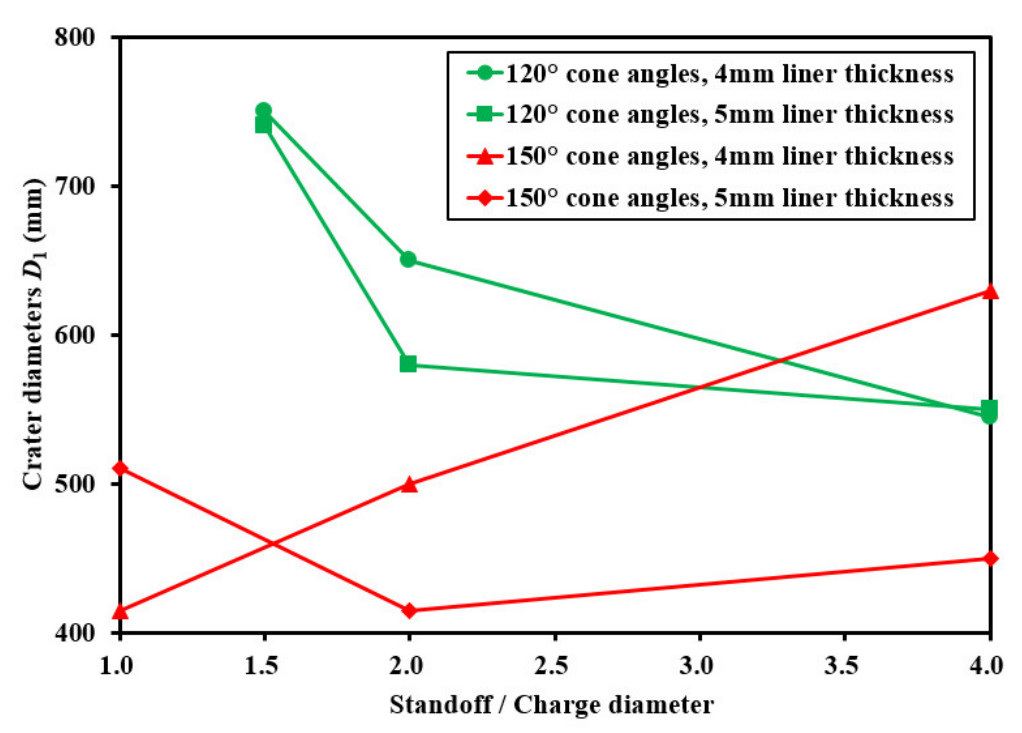


Figure 8: Variation laws of D<sub>1</sub> with standoffs.

#### 3.2. Results of Hole Diameter D<sub>2</sub>

From Table 2 and Fig. 9 we can find that, in the case of 120° cone angle, the variation of hole diameter with the increase of standoff is small. For the same standoff, the hole diameter formed by shaped charge with 5mm liner wall thickness, comparing to 4mm, is larger. When the liner wall thicknesses are 4mm and 5mm respectively, the corresponding maximum values of hole diameter are 0.5D and 0.6D. In the case of standoff between 1D and 2D, hole diameter formed by shaped charge of 150° cone angle vary widely with the standoff changing. It is opposite to the standoff higher than 2D, in which the hole diameter almost keep unchangeable even though the standoff vary. For the same standoff, the hole diameter formed by shaped charge with 4mm liner wall thickness, comparing to 5mm, is larger. When the liner wall thicknesses are 4mm and 5mm respectively, the corresponding maximum values of hole diameter are 3D and 2D. For the same charge diameter, the values of hole diameter formed by EFP with 150° cone angle were much larger than JPC with 120° cone angle.

Table 2: Experimental results of hole diameter with different cone angles and liner wall thicknesses under different standoffs (mm)

Cone angle (°) Thickness (mm)		Standoff					
8		1D	1.5D	2D	4D		
120	4	_	35×35	30×30	28×28		
	5	_	40×40	40×40	45×45		
150	4	140×140	_	200×200	210×210		
	5	130×130		100×100	140×140		

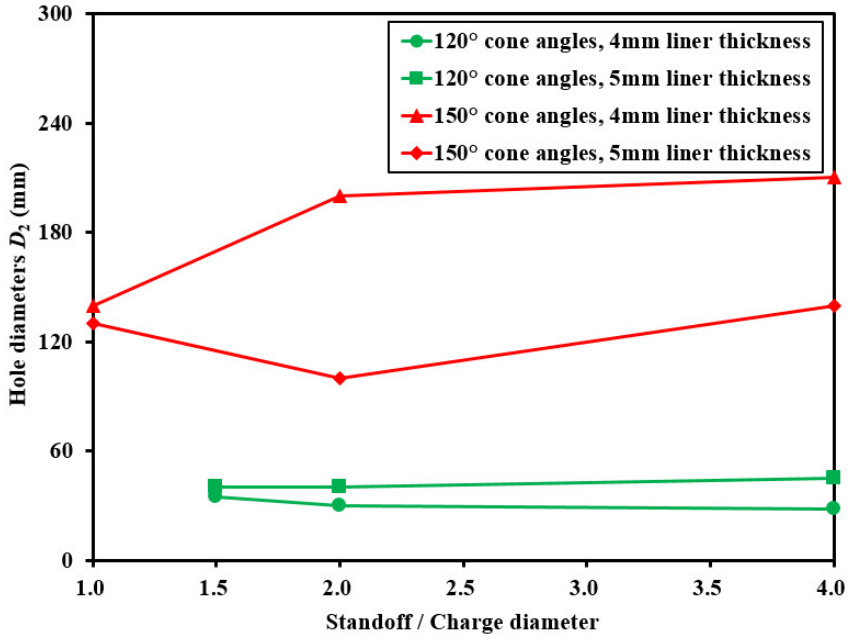


Figure 9: Variation laws of D<sub>2</sub> with standoffs.

# 3.3. Results of Crater Depth H<sub>1</sub>

Table 3 and Fig. 10 illustrates that, for four kinds of standoffs (1D, 1.5D, 2D and 4D), the crater depth caused by shaped charge with 120° cone angle decreases with the increase of standoff. For the same standoff, the crater depth formed by shaped charge with 5mm liner wall thickness, comparing to 4mm, is larger. The maximum value of crater depth is 1.8D for both 4mm and 5mm liner wall thicknesses. The crater depth formed by shaped charge with 150° cone angle decreases with the increase of standoff. In the case of liner wall thicknesses are 4mm and 5mm, the corresponding maximum values of crater depth are 1.4D and 1.5D respectively.

Table 3: Experimental results of crater depth with different cone angles and liner wall thicknesses under different standoffs (mm)

Cone angle (°) Thickness (mm)			·	Standoff	
		1D	1.5D	2D	4D
120	4	_	125	110	85
	5	_	125	117	115
150	4	98	_	96	86
	5	105	_	90	88

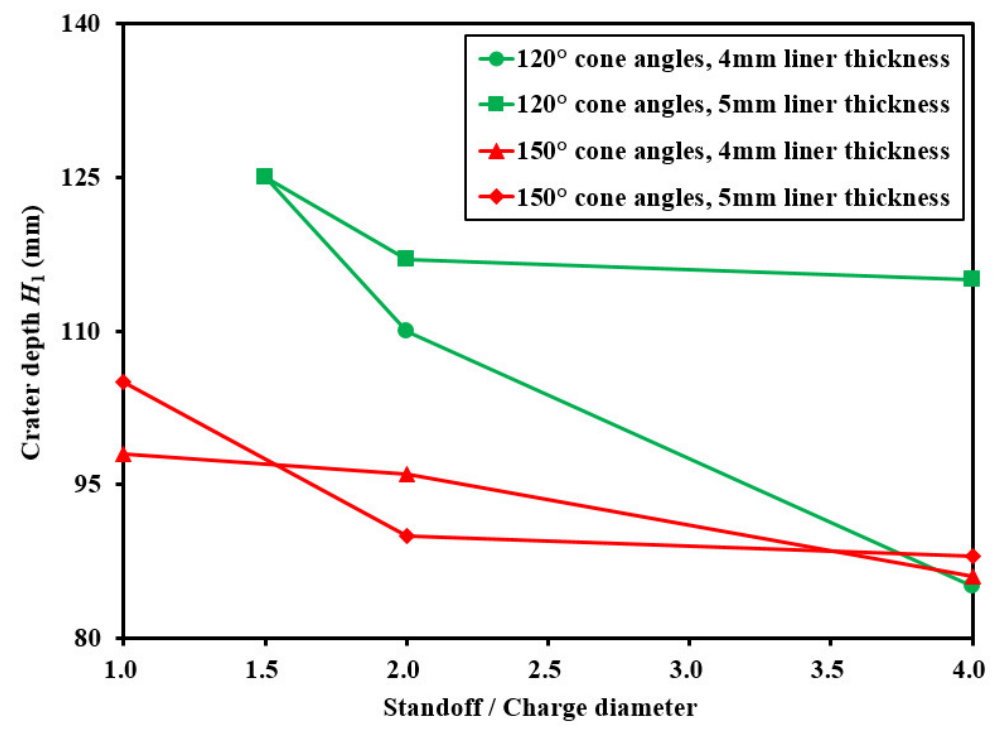


Figure 10: Variation laws of H<sub>1</sub> with standoffs.

#### 3.4. Results of Penetration Depth H

It is clear from Table 4 and Fig. 11 that, when standoff is higher than or equal to 2D, the penetration depth caused by the shaped charge with 120° cone angle decreases with the increase of standoff. The JPC breaks up with standoff high, so the penetration depth of JPC reduces. For the same standoff, the penetration depth caused by the shaped charge with 4mm liner wall thickness is larger than 5mm liner wall thickness. The penetration depth caused by the shaped charge with 150° cone angle varies slightly with the standoff increasing. For the same standoff, the penetration depth caused by the shaped charge with 120° cone angle (JCP) were larger than 150° cone angle (EFP).

Table 4: Experimental results of penetration depth with different cone angles and liner wall thicknesses under different standoffs (mm)

Cone angle (°) Thickness (mm)				Standoff		
		1D	1.5D	<b>2D</b>	<b>4D</b>	
120	4	_	280	295	265	
	5	_	215	206	170	
150	4	98	_	96	86	
	5	105	_	90	88	

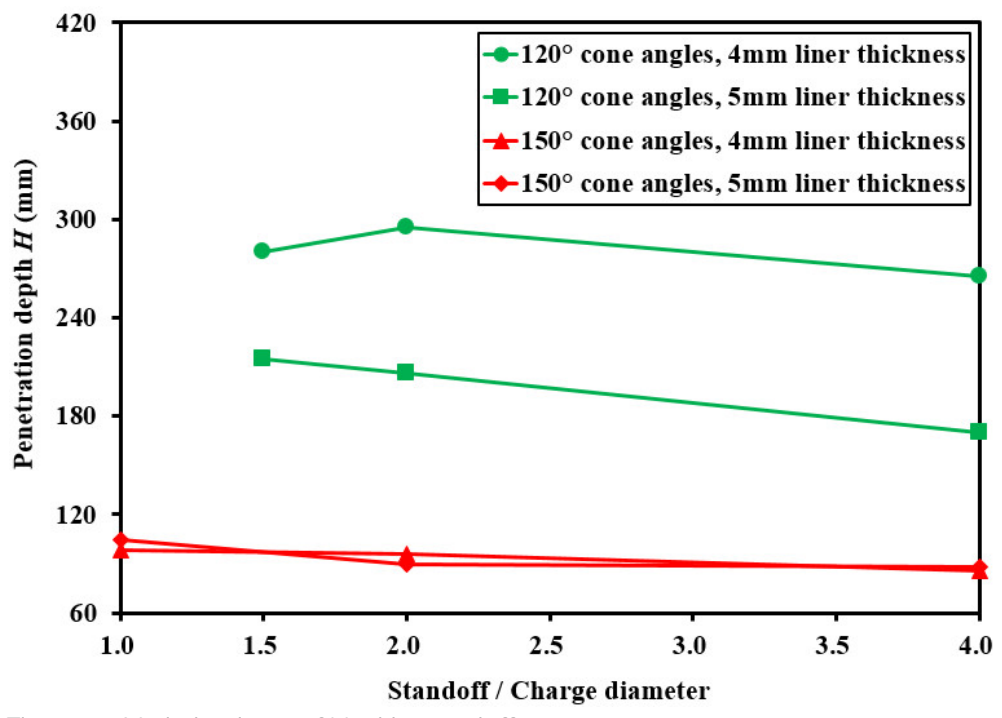


Figure 11: Variation laws of H with standoffs.

#### 4. THE RESULTS OF CHARGE DIAMETER 65MM

#### 4.1. Results of Crater Diameter D<sub>1</sub>

From Table 5 and Fig. 12 we can see that, when the shaped charge with length to diameter ratios are 0.8 and 1.4, the corresponding maximum values of crater diameter are 8.7D and 9.4D respectively. In 1D standoff, the crater diameter caused by the shaped charge with length to diameter ratio of 1.4 is larger than 0.8. However, the crater diameter formed by the shaped charge with length to diameter ratio of 1.4 is smaller than that of 0.8 for 2.5D standoff.

Table 5: Experimental results of crater diameter with different length to diameter ratios and liner wall thicknesses under different standoffs (mm)

L/D Thickness (mm)				Stando	off	
	,	0.5D	1D	1.5D	2D	2.5D
0.8	3	470×520	510×540	300×400	400×480	500×630
	1.8~1.3	470×490	480×510	500×510	460×510	540×550
1.4	3	460×510	600×620	400×450	480×500	420×440
	1.8~1.3	400×420	580×600	500×500	560×650	330×400

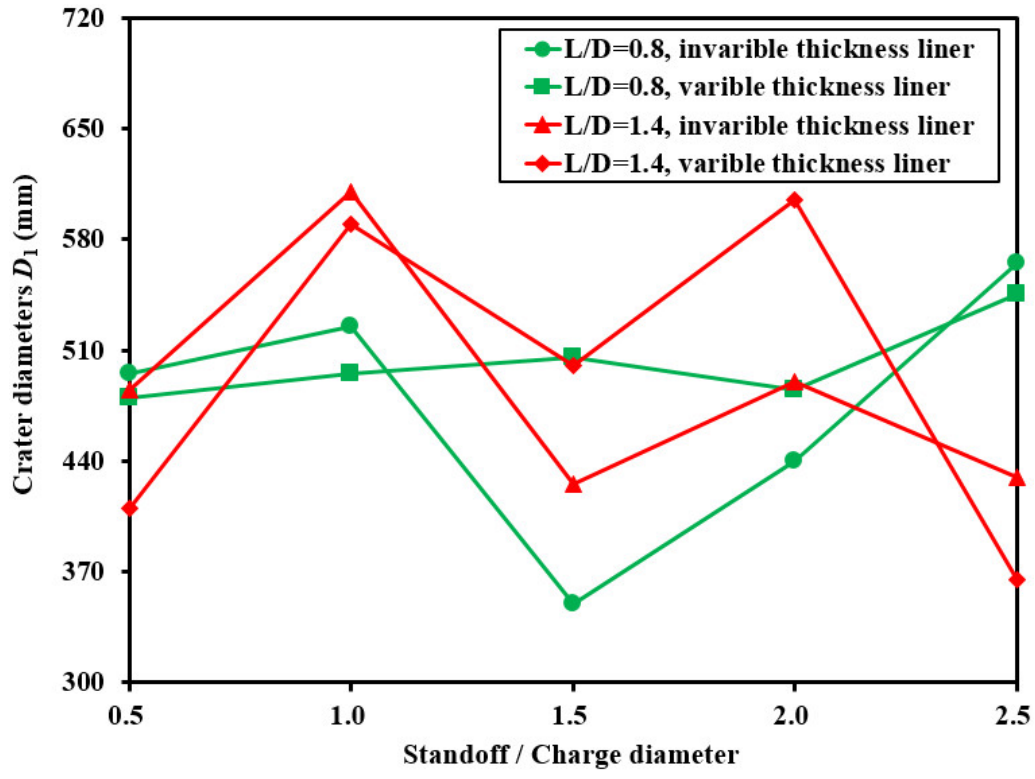


Figure 12: Variation laws of D<sub>1</sub> with standoffs.

#### 4.2. Results of Hole Diameter D<sub>2</sub>

Table 6 and Fig. 13 illustrate that, for standoff higher than or equal to 1.5D and length to diameter ratio of 1.4, the variation laws of hole diameter caused by different liner wall thicknesses are similar. In the case of length to diameter ratio of 0.8, the maximum values of hole diameter are 0.7D and 0.6D for invariable and variable liner wall thicknesses. When length to diameter ratio is 1.4, the maximum values of hole diameter for invariable and variable cases are 0.8D and 0.5D.

Table 6: Experimental results of hole diameter with different length to diameter ratios and liner wall thicknesses under different standoffs (mm)

L/D Thickness (mm)		Standoff					
	,	0.5D	1 <b>D</b>	1.5D	<b>2D</b>	2.5D	
0.8	3	30×30	40×50	40×40	20×25	35×40	
	1.8~1.3	40×40	35×40	35×40	30×30	25×25	
1.4	3	20×20	40×60	30×30	30×30	25×30	
	1.8~1.3	25×25	30×30	30×35	30×40	30×30	

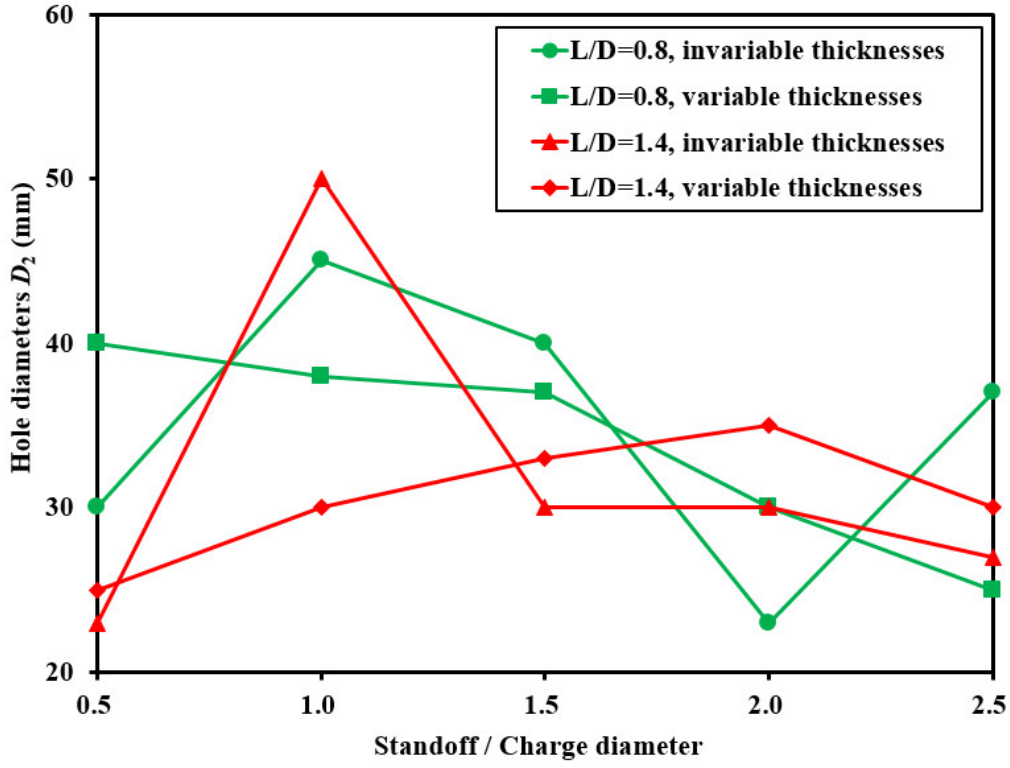


Figure 13: Variation laws of D<sub>2</sub> with standoffs.

#### 4.3. Results of Crater Depth H<sub>1</sub>

It is obvious from Table 7 that, when the length to diameter ratio is 0.8, the maximum values of crater depth are 1.8D and 1.4D for two kinds of liner wall thicknesses. The maximum values of crater depth are 1.8D and 1.7D, when length to diameter ratio is 1.4 for invariable and variable liner wall thicknesses. In the condition of different charge ratio of length to diameter, the maximum value of crater depth caused by shaped charge with invariable liners wall thickness is larger than it caused by the shaped charge with variable liners wall thickness. When the charge ratio of length to diameter is identical, in the same standoff (except 1D), the crater depth formed by shaped charge of invariable liners wall thickness is larger than it caused by the shaped charge of variable liners wall thickness as shown in Fig. 14.

Table 7: Experimental results of crater depth with different length to diameter ratios and liner wall thicknesses under different standoffs (mm)

L/D Thickness (mm)				f		
	, ,	0.5D	1D	1.5D	<b>2D</b>	2.5D
0.8	3	100	75	120	105	90
	1.8~1.3	90	90	90	85	80
1.4	3	115	115	110	105	100
	1.8~1.3	75	110	110	85	78

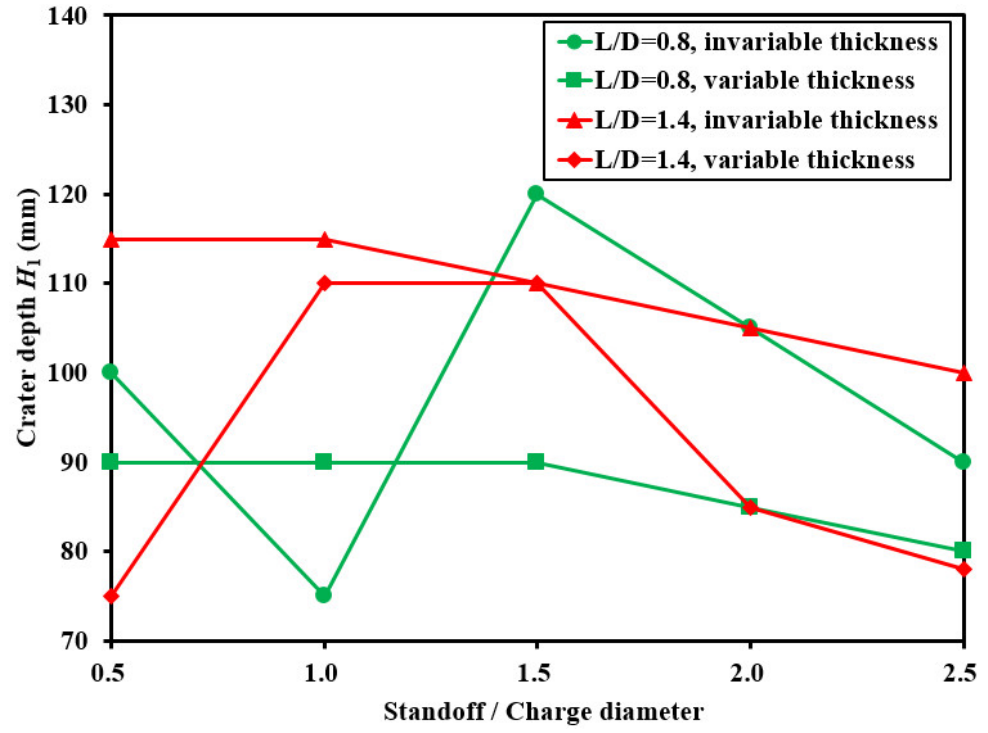


Figure 14: Variation laws of H<sub>1</sub> with standoffs.

### 4.4. Results of Penetration Depth H

Table 8 illustrates that, when the standoff do not exceed 1.5D, penetration depth increases with the increase of standoff. The lower the standoff is, the larger the JPC diameter has. Most energy released is used to expand the hole diameter, which leads to decreasing penetration depth. When the standoff is between 1.5D and 2.5D, the penetration depths of different projectiles are almost the same as shown in Fig. 15.

Table 8: Experimental results of penetration depth with different length to diameter ratios and liner thicknesses under different standoffs (mm)

L/D Thickness (mm)				Standof	Î	
	,	0.5D	1 <b>D</b>	1.5D	<b>2</b> D	2.5D
0.8	3	140	155	405	419	420
	1.8~1.3	110	205	407	410	409
1.4	3	145	185	415	400	400
	1.8~1.3	175	224	406	413	410

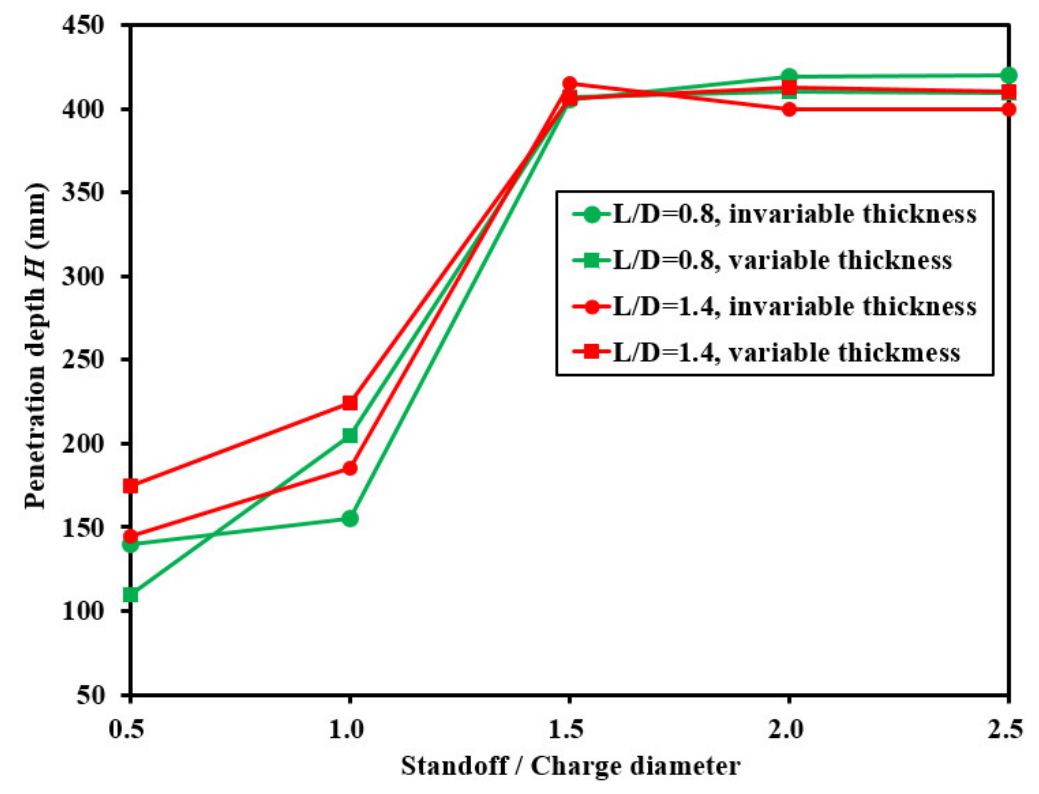


Figure 15: Variation laws of H with standoffs.

#### 5. NUMERICAL RESULTS AND ANALYSIS

In Section 5, REMAP technology of software AUTODYN was used to investigate the formation and penetration of shaped charge. Firstly, the forming process of the shaped charge was simulated to obtain the data of the projectile at different time. Then, the calculation result was mapped to the concrete target model for the penetration calculation. Euler's method was applied to simulate the shaped charge formation and the mesh size was set as 1mm. The JWL equation of state was introduced to describe the composition B and the shock model was used to simulate the steel shell and liner. The simulation model of D=70mm and cone angle 120° was shown in Fig. 16(a). The Fig. 16(b) was the simulation model of D=65mm and L=94mm.

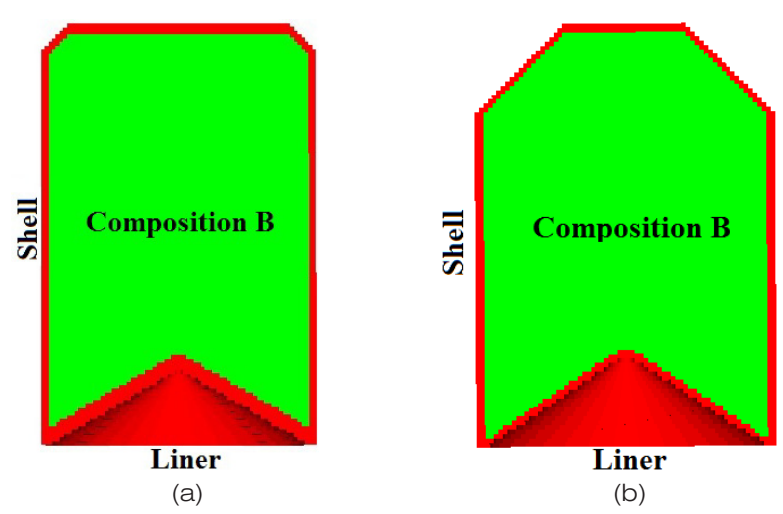


Figure 16: The simulation models of different charge diameters; (a) D=70mm. (b) D=65mm.

In the progress of penetration calculation, the Lagrange approach is used. The strength model of concrete is von Mises model and the EOS of concrete is polynomial which described as:

$$P(\rho,e) = A_1 \mu + A_2 \mu^2 + A_3 \mu^3 + (B_0 + B_1 \mu) \rho_0 e$$
 (1)

where,  $\mu = \left(\frac{\rho}{\rho_o} - 1\right)$  is relative volume change;  $\rho_o$  is initial material density; e is internal energy per unit mass;  $A_1$ ,  $A_2$ ,  $A_3$ ,  $B_0$  and  $B_1$  are material constants. The values of these are listed in Table 9.

The porous equations of state, Drucker-Prager constitutive equation and Hydro failure model were introduced to describe the pebble. The remapped initial model were shown in Fig. 17. Local mesh refinement technology was implemented in the target. The transmit boundary condition was used between different target layers.

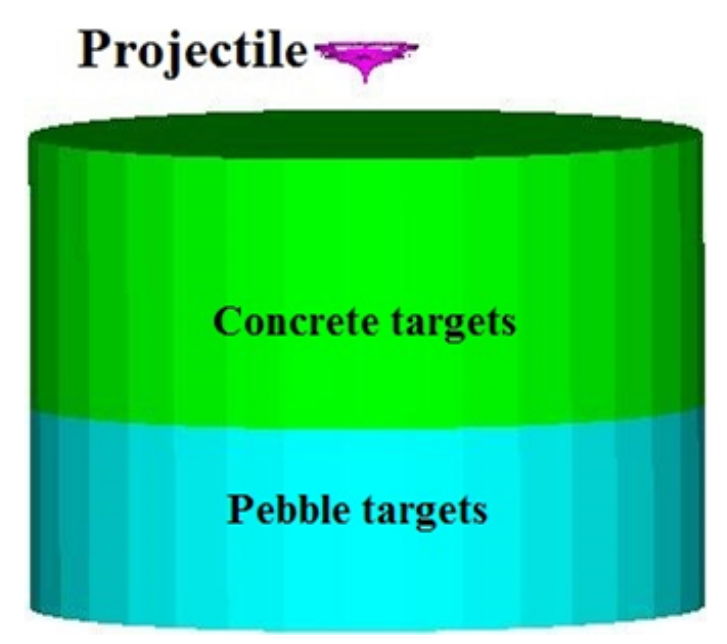


Figure 17: Simulation results of shaped charge remapped into Lagrange approach.

## 5.1. Numerical results and analysis of charge diameter of 70mm

As showed in Fig. 18, the liner of shaped charge with 120° cone angles moves inward and generating shaped charge jet, the liner of shaped charge with 150° cone angles overturns and generating explosively formed projectile (EFP). It indicated that the cone angle is an important factor for the shaped charge formation. In the condition of cone angles be the same, the projectiles' shape of different liners wall thickness is similar and the velocity of projectiles formed by thicker liners is lower. Compared with projectiles formed by charge diameter of 65mm, in the same standoff, the diameter of projectiles formed by charge diameter of 70mm is bigger and the velocity is higher. That lead to the projectiles formed by charge diameter of 70mm cannot be though the concrete layer.

Table 10 shows the comparison between numerical results and experimental results of penetration depth. The maximum error of 70mm charge diameter is only 9.5%. It demonstrates that the numerical techniques such as boundary conditions, mesh size, equations of state and so on are reasonable in this paper.

# 5.2. Numerical results and analysis of charge diameter of 65mm

Table 11 shows the comparison between numerical results and experimental results of penetration depth. It illustrates that the maximum errors do not exceed 7.9% for 65mm charge diameter. Fig. 19 shows the numerical results of two kinds of length to diameter ratios (L/D=0.8 and 1.4) and the invariable and variable liner wall thicknesses in 2D standoff. The hole diameter tends to be narrow obviously in the location P1. The JPC composes of jet and slug, in which the velocity gradient of jet is larger. Therefore, it becomes slender with the increase of the penetration depth. The slug diameter is almost invariant due to its small velocity gradient, thus the wider part of hole diameter in the location P1 is mainly caused by slug. The interfacial effect exists obviously when shaped

Table 10: Comparison between numerical and experimental results of penetration depth for 70mm charge diameter

Standoff	Cone angle (°)	Thickness (mm)	Experimental value (mm)	Numerical value (mm)	Error (%)
1D	150	4.0	98	105	7.1
		5.0	105	115	9.5
1.5D	120	4.0	280	297	6.1
		5.0	215	203	-5.6
	120	4.0	295	320	8.5
2D		5.0	206	219	6.3
	150	4.0	96	90	-6.3
		5.0	90	97	7.8
	120	4.0	265	283	6.8
4D		5.0	170	155	-8.8
	150	4.0	86	92	7.0
		5.0	88	95	8.0

Table 11: Comparison between numerical and experimental results of penetration depth for 65mm charge diameter

Standoff	L/D	Thickness (mm)	Experimental value (mm)	Numerical value (mm)	Error (%)
	0.8	3.0	140	151	7.9
0.5D		1.8~1.3	110	107	-2.7
	1.4	3.0	145	154	6.2
		1.8~1.3	175	187	6.9
	0.8	3.0	155	167	7.7
1D		1.8~1.3	205	213	3.9
	1.4	3.0	185	172	-7.0
		1.8~1.3	224	235	4.9
	0.8	3.0	405	411	1.5
1.5D		1.8~1.3	407	411	1.0
	1.4	3.0	415	420	1.2
		1.8~1.3	406	400	-1.5
	0.8	3.0	419	434	3.6
2D		1.8~1.3	410	419	2.2
	1.4	3.0	400	379	-5.3
		1.8~1.3	413	405	-1.9
	0.8	3.0	420	425	1.2
2.5D	0.0	1.8~1.3	409	412	1.0
	1.4	3.0	400	410	2.5
		1.8~1.3	410	395	-3.7

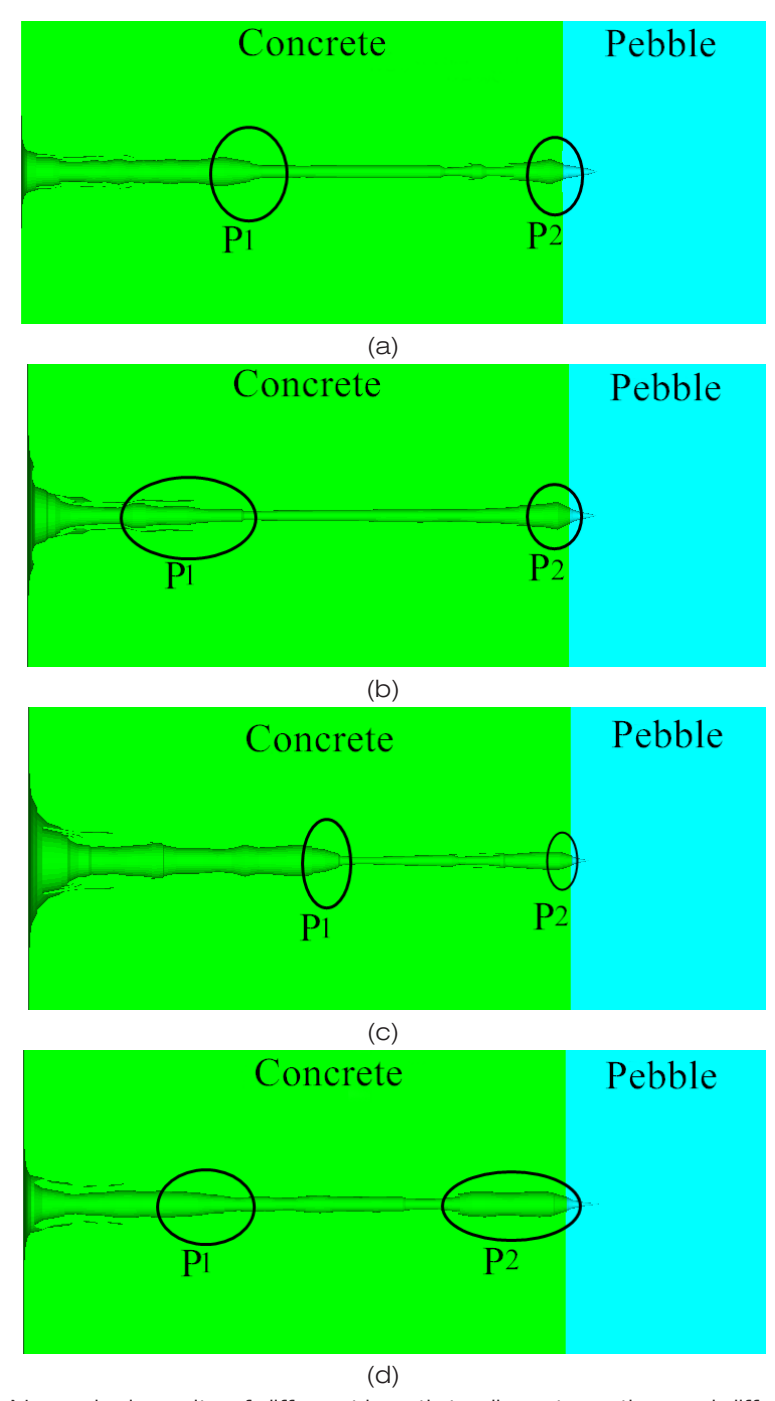


Figure 19: Numerical results of different length to diameter ratios and different liner wall thicknesses in 2D standoff; (a) L/D=0.8 and invariable thickness. (b) L/D=0.8 and variable thickness. (c) L/D=1.4 and invariable thickness. (d) L/D=1.4 and variable thickness.

charge penetrates into multi-layer targets, which can be found in the location P2. In the neighbor of the interface between concrete and pebble, the penetration diameter on the concrete side enlarges locally. The shock impedance of pebble is higher than concrete, hence partial JPC flows along the radial direction in the concrete side, which makes the part close to the concrete and pebble interface become large.

#### 6. CONCLUSION

Experiments and numerical simulations for shaped charge penetrating into multi-layer targets were performed in this paper. The influence of cone angles, liner wall thicknesses, length to diameter ratios and charge diameters with different standoffs on crater diameter, hole diameter, crater depth and penetration depth were analyzed, and some conclusions are given as follows:

- 1. A large number of experimental models performed in this paper to investigate penetration into multi-layer targets by shaped charge are also simulated numerically. The numerical results are in good agreement with the experimental results.
- 2. Different formation mechanisms can lead to obvious differences between JPC and EFP for penetrating into multi-layer targets. For the same charge diameter, the values of hole diameter formed by EFP were much larger than JPC. However, for the same standoff, the penetration depth caused by JCP were larger than EFP.
- 3. The formation laws of crater diameter, hole diameter, crater depth and penetration depth with the variations in cone angle, liner wall thickness, length to diameter ratio, charge diameter and standoff are different. Therefore, it is of great significance to take into comprehensive consideration all the impact factors to optimize the design of shaped charge.
- 4. The interfacial effect is obvious in the penetration of shaped charge into multi-layer targets. Due to the shock impedance of pebble is higher than concrete, the JPC radial flow emerges in the concrete side when the JPC just penetrates into the pebble, which causes hole diameter to expand.

#### **ACKNOWLEDGMENTS**

This research is supported by the National Natural Science Foundation of China under grants 11325209, 11521062 and Science Challeng Project, No. TZ2016001.

#### **REFERENCES**

- [1] Birkhoff, G., et al., Explosives with lined cavities. Journal of Applied Physics, 1948. 19(6): p. 563-582.
- [2] Allison, F. E., and Vitali, R., A new method of computing penetration variables for shaped charge jets. Army Ballistic Research Lab Aberdeen Proving Ground MD, No. BRL-1184, 1963.
- [3] Tate, A., A theory for the deceleration of long rods after impact. Journal of the Mechanics and Physics of Solids, 1967. 15(6): p. 387-399.
- [4] Tate, A., Long rod penetration models—Part II Extensions to the hydrodynamic theory of penetration. International Journal of mechanical sciences, 1986. 28(9): p. 599-612.
- [5] Chou, P.C., and Foster, J.C., Theory of penetration by jet of non-liner velocity and in layered targets. In Proceedings of the 10th International Symposium on Ballistics, California, 1987.

- [6] Szendrei, T., Analytical model of crater formation by jet impact and its application to calculation of penetration curves and holes profiles. In Proceedings of the 7th International Symposium on Ballistics, Netherlands, 1983.
- [7] Held, M., Verification of the equation for radial crater growth by shaped charge jet penetration. International journal of impact engineering, 1995. 17(1-3): p. 387-398.
- [8] Wang, J., Wang, C., and Ning, J.G., Theoretical model for shaped charge jets penetration and cavity radius calculation. Engineering Mechanics, 2009, 26(4): p. 21-26.
- [9] Meyer, C S., Numerical Investigation of Impact Condition Effects on Concrete Penetration. Dynamic Behavior of Materials, 2015. 1: p. 285-293.
- [10] Resnyansky, A. D., and Weckert, S., A., Damage of Two Concrete Materials due to Enhanced Shaped Charges. Dynamic Behavior of Materials, 2015. 1: p. 267-277.
- [11] Nicolaides, D., et al., Experimental field investigation of impact and blast load resistance of Ultra High Performance Fibre Reinforced Cementitious Composites (UHPFRCCs). Construction and Building Materials, 2015. 95: p. 566-574.
- [12] Pincosy, P.A., and Murphy, M.J., Calculated concrete target damage by multiple rod impact and penetration. In Proceedings of the 23rd International Symposium on Ballistics, Spain, 2007.
- [13] Xiao, Q. Q., et al., Penetration research of jacketed jet into concrete. International Journal of Impact Engineering, 2013. 54: p. 246-253.
- [14] Wang, C., Wang, W.J., and Ning, J.G., Investigation on shaped charge penetrating into concrete targets. Chinese Journal of Theoretical and Applied Mechanics, 2015. 47(4): p. 672-686.